ANALYSIS OF IONIZATION BEHAVIOR AND THERMODYNAMIC PARAMETERS OF SCHIFF BASES UNDER SOLVENT EFFECTS: AN ELECTRICAL STUDY WITH MOLECULAR DOCKING-BASED BIOLOGICAL ACTIVITY EVALUATION

A.A. Aldabagh*, F.H.M. Altaiea

Department of Chemistry, College of Education for Pure Sciences, University of Mosul, Mosul, Iraq
**e-mail: amina.24esp33@student.uomosul.edu.iq, Tel: +9647706722622*

Received 29.03.2026
Accepted 05.06.2026

Abstract: *This study reports the synthesis of three phenolic Schiff bases derived from 4-aminobenzophenone with hydroxyl groups at ortho-, meta-, and para- positions. Structural characterization is performed using UV-Vis, FT-IR, and ^{1}H-NMR spectroscopy. The ionization constants (Ka) are determined over a temperature range of 293 - 333 K using electrical conductivity measurements. Results indicate that acidity increases with temperature while maintaining a consistent Ka order of magnitude. Thermodynamic analysis reveals that the ionization process is non-spontaneous ($\Delta G > 0$), endothermic ($\Delta H > 0$), and accompanied by a decrease in entropy ($\Delta S < 0$). The effect of thermal variation on equivalent conductivity values at infinity dilution was also analyzed. The study shows a decrease in Ka values when water was replaced with absolute ethanol. Biological activity tests demonstrated effectiveness against both Gram-positive (Staphylococcus aureus and Streptomyces lavendulae) and Gram-negative (Escherichia coli), with compound 2-(((4-aminophenyl)(phenyl)methylene)amino)phenol exhibiting the highest inhibition. Molecular docking analysis supports experimental findings by confirming favorable interactions between synthesized compounds and biological targets.*

Keywords: *Schiff bases, conductivity, ionization constant Ka, thermodynamic, biological activity, molecular docking.*

Introduction

Schiff bases are organic compounds characterized by the presence of an imine group (C=N), resulting from the condensation of aldehydes or ketones with primary amines [1]. An important feature of these compounds is their ability to coordinate with metal ions and form stable complexes with diverse physical and chemical properties [2]. Variations in the nature and location of substituents can greatly affect the spatial and electronic environment of the imine system, thereby affecting the chemical reactivity and biological performance of these derivatives [3]. As a result, Schiff bases have been subjected to extensive studies for their antibacterial, antifungal, anticancer, and antioxidant activities [4]. Their pharmaceutical relevance has been highlighted in recent studies that confirm its value as a promising biological structure [5]. In addition, advanced systems based on the Schiff base have demonstrated enhanced antimicrobial performance [6]. Among aromatic systems, benzophenone derivatives represent an important class characterized by photochemical stability and efficient light absorption [7]. These compounds also exhibit versatile behavior in functional applications [8]. Furthermore, benzophenone derivatives have attracted considerable attention because of their biological and environmental relevance [9]. The incorporation of aminophenol molecules can increase reactivity through hydrogen bonding and electronic delocalization [10]. This effect is supported by studies showing that Schiff bases of aminophenol have enhanced biological activity [11]. To quantify pKa values is not only a chemical need; it is an essential step in understanding the ways in which Schiff base derivatives interact with bioactive targets [12, 13]. pKa values can be determined under equilibrium conditions using conductivity measurements, a reliable approach for weak electrolytes [14]. In pharmaceutical systems, ionization properties become essential for drug absorption, distribution, metabolism, and excretion [15]. The acid dissociation constant (Ka) quantitatively describes the equilibrium between the ionized and non-ionized forms of a substance, reflecting its intrinsic tendency to donate or accept protons in solution. This parameter is particularly important for weak electrolytes, including Schiff bases, whose physicochemical and

biological properties are strongly influenced by their ionization behavior [16, 17]. Since pKa is inherently temperature-dependent, its variation with temperature can be exploited to derive important thermodynamic parameters, including the Gibbs free energy (ΔG), enthalpy (ΔH), and entropy (ΔS) of ionization, thereby providing valuable insights into the energetics and mechanism of the ionization process [18]. Molecular docking technology has become an important computational method to predict interaction of protein compounds and to study biological activity at a molecular scale [19]. It helps identify key binding interactions, such as hydrogen bonding and hydrophobic contacts, which are required for stable ligand attachment at the active site [20].

The present research emphasizes the preparation of Schiff bases (derived from benzophenone A1-A3), conductivity based measurement of pKa over the temperature range 293-333 K, thermodynamic analysis and solvent effect, biological activity, and molecular simulation studies of the target protein (PDB: 1KMZ). It serves to clarify the connection between molecular structure and ionization behavior, and biological activity.

Experimental part

Materials and Methods. All starting materials, including 4-aminobenzophenone, ortho-, meta-, and para-aminophenol, and solvents (absolute ethanol and glacial acetic acid), were of analytical grade. They were purchased from Sigma-Aldrich, BDH, and Fluka and used as received without further purification. The progress of the reactions is monitored using Thin-Layer Chromatography (TLC). The melting points of the synthesized Schiff bases were determined using a Stuart SMP (Bibby Scientific Limited) digital device. Electronic spectra were recorded on a Shimadzu UV-Visible 1601 spectrophotometer. FT-IR spectra are obtained using a Bruker Alpha spectrometer in the range of 4000–400 cm^{-1} via the Attenuated Total Reflectance (ATR) technique. The ^{1}H-NMR spectra were recorded on a Varian Agilent 500 Technologies spectrometer (500 MHz, USA) using DMSO-d_6 as a solvent. Electrical conductivity was measured using a Wissenschaftlich-Technische Werkstatten conductivity meter, and temperatures were precisely maintained using a Memmert water bath (model L200, Searle).

Preparation of Schiff bases. Schiff bases are prepared by mixing equivalent molar amounts through the reaction of 1.97 g at a concentration of 0.01 M of 4-aminobenzophenone compound dissolved in 15 ml of absolute ethanol with 1.091 g at a concentration of 0.01 M of aminophenol derivatives (o, m, p-aminophenol) dissolved in the same solvent, then placed in a conical flask of 100 ml equipped with a magnetic stirrer, and (2-3) drops of glacial acetic acid are added to the reaction mixture as a catalyst, and the mixture is stirred continuously for 10 hours at a temperature between 70 and 80°C. The reaction is monitored by TLC using hexane 4: ethyl acetate 1. After the reaction was complete, the contents of the flask were transferred to a beaker, the reaction mixture was cooled with ice, and the resulting precipitate was filtered and washed several times with hot absolute ethanol to recrystallize and remove impurities [21, 22]. We include Scheme 1 as a typical example for preparing Schiff bases for the compounds under study (A1, A2, and A3). The main physicochemical properties of prepared compounds are listed in Table 1.

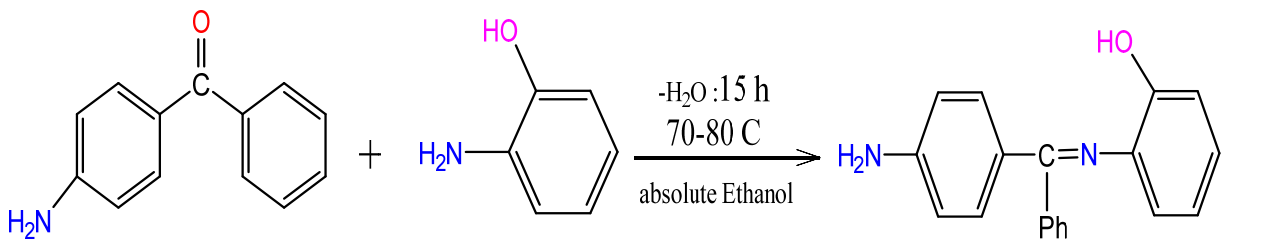

(4-aminophenyl)(phenyl)methanone 2-aminophenol 2-(((4-aminophenyl)(phenyl)methylene) amino)phenol

Scheme 1. Preparation of the ketonic Schiff base derivative

Table 1. Structural formulas, melting points and colour of the prepared compounds

Symbol	Compound	Structural Formula	Melting Point, C°	Colour
A1	2-(((4-aminophenyl)(phenyl) methylene)amino) phenol	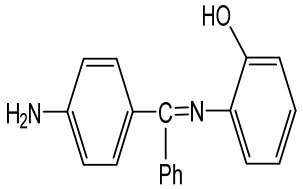	111-112	Brown
A2	3-(((4-aminophenyl)(phenyl) methylene)amino) phenol	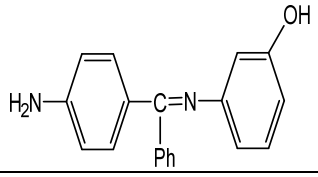	100-102	Light purple
A3	4-(((4-aminophenyl)(phenyl) methylene)amino) phenol	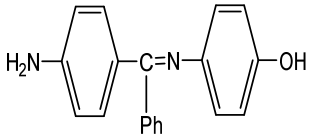	115-116	Dark purple

Results and discussion

The three prepared Schiff bases were studied, and their structural formulas were characterized and confirmed using various physicochemical techniques below.

UV-Visible Spectra. UV-visible spectra were recorded in the (200 – 450 nm) range at a concentration of (10^{-4} M). Measurements were performed in a polar solvent, absolute ethanol, and in a weakly polar solvent, dichloromethane (CH_2Cl_2). The type of electronic transition was identified based on the molar absorptivity values (ε_{max}), as summarized in Table 2.

Table 2. Significant absorption maxima in the UV–Vis spectra of the Schiff bases measured in ethanol and dichloromethane

Symbol	Ethanol solvent			dichloromethane solvent			Transition type	$\overline{\Delta v}$ (cm)
	λ_{max} (nm)	A	ε_{max} $Lmol^{-1}$ cm^{-1}	λ_{max} (nm)	A	ε_{max} $Lmol^{-1}$ cm^{-1}		
A1	338	2.894	28940	316	1.465	14650	$\pi \rightarrow \pi^*$	-2059.7
A2	322	2.527	25270	304	2.069	20690	$\pi \rightarrow \pi^*$	-1838.8
A3	330	1.630	16300	366	1.803	18030	$\pi \rightarrow \pi^*$	+2980.6

Table 2 shows that the values of the molar absorption coefficient were greater than 1000 $Lmol^{-1}cm^{-1}$, indicating that the electron transition was of the ($\pi \rightarrow \pi^*$) type. Although (C=N) and (NH_2) groups exist that allow ($n \rightarrow \pi^*$) transitions, the high absorption intensity (ε_{max}) greater than (1000) indicates the dominance of ($\pi \rightarrow \pi^*$) transitions, while the weak ($n \rightarrow \pi^*$) transitions disappear due to spectral overlapping and the polar solvent effect [23, 24].

Infrared (IR) Spectra. IR spectra were recorded for the prepared compounds in the solid state. The results showed a broad absorption band in the region (3416–3418 cm^{-1}), attributed to hydroxyl (OH) group vibrations. The breadth of this band may indicate the presence of hydrogen bonds. A weak absorption band was also observed in the region (3043–3052 cm^{-1}), attributed to aromatic (C–H) vibrations. Additionally, a distinct band appeared in the range (1626–1627 cm^{-1}), belonging to the imine (C=N) group, confirming the formation of Schiff bases. Furthermore, a characteristic pairing of symmetric and asymmetric (NH_2) absorption bands was observed in the studied compounds within

the range (3302–3333 cm^{-1}). Overall, the UV and IR spectra were consistent with those reported in previous studies [23, 25]. As shown in Table 3 and Fig. 1.

Table 3. Infrared (IR) spectra of the synthesized Schiff bases

Symbol	Positive peak numbers (cm^{-1})			
	υ C=N	υ C-H	υ OH	υ NH_2
A1	1627(S)	3052(W)	3416(m)	3333(W) 3302(S)
A2	1627(S)	3043(W)	3418(S)	3332(S) 3218(m)
A3	1626(S)	3050(W)	3417(m)	3333(S) 3218(m)

S=Sharp, w =Weak, m =medium.

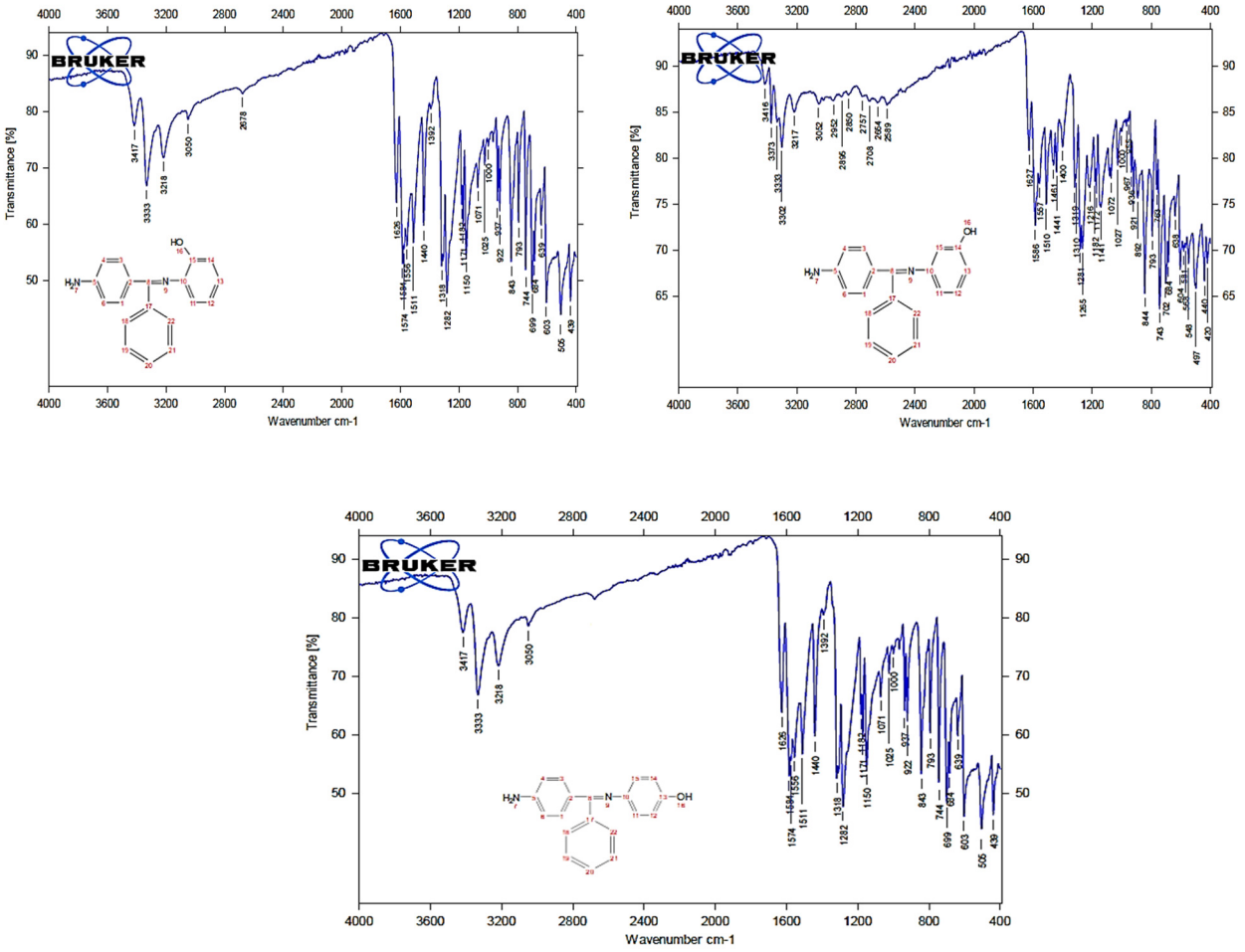

Fig. 1. IR spectra for compounds A1, A2, and A3

H^1-NMR Spectra. The proton nuclear magnetic resonance (^{1}H-NMR) spectrum of compound (A2) was recorded in DMSO-d_6 solvent at a frequency of 400 MHz. These spectra provide information about the chemical environment of the protons, including the aromatic and hydroxyl groups, for the prepared compound [26]. An illustrative example of the remaining rules is shown in the Figure 2. The spectrum gave δ=10.38 ppm (S, 1H, -OH); δ=8.91 ppm (S, 1H, -CH=N-); δ=6.03-7.47 ppm (m, Ar-H); δ=4.93 ppm (2H, -NH_2); δ=3.51 ppm (H_2O), and δ=2,51 ppm (DMSO-d_6).

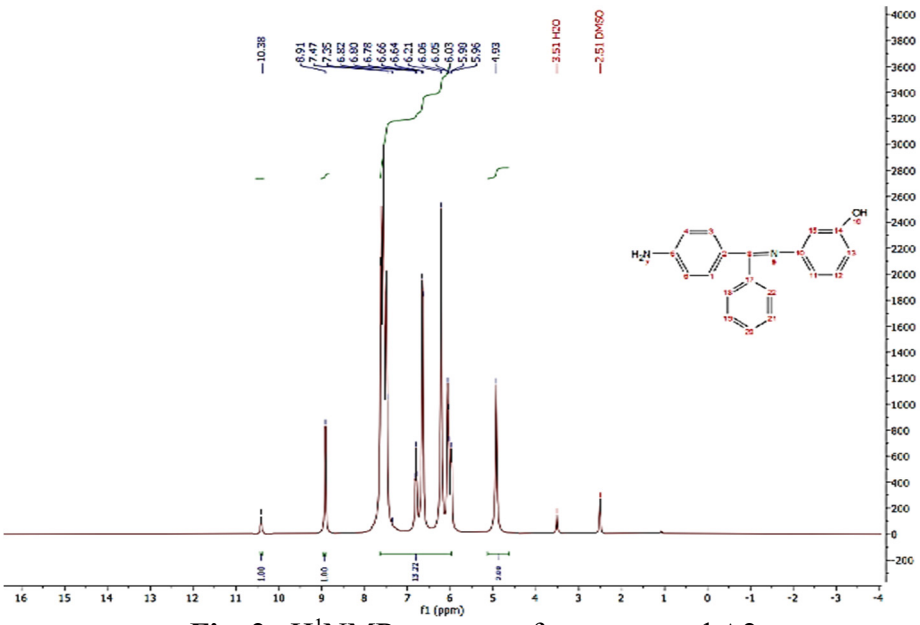

Fig. 2. H[1]NMR spectrum for compound A2

Method of electrical connection. For the purpose of measuring electrical conductivity, standard solutions of each Schiff base were prepared at a concentration of 10^{-3} M. This was done by adding (10 mL) of absolute ethanol to dissolve the Schiff base, then completing the volume with electrically conductive water until a final volume of 50 mL was reached for each solution. By dilution, four solutions were prepared at different concentrations (0.2×10^{-3} – 10^{-3} M) at different temperatures within the range of 293–333 K. Subsequently, sodium salts of the prepared Schiff bases were prepared using the conventional titration method with phenolphthalein indicator, to a concentration of 10^{-3} M of each prepared base. Further dilution was then carried out to obtain five solutions of different concentrations, with a final volume of 50 mL, and their electrical conductivity was measured. Temperatures were controlled within the range of 293–333 K using a water bath equipped with a thermostat. The electrical conductivity method was used to determine the ionization constants of the studied bases (A1, A2, and A3). For this purpose, the equivalent conductivity (Λ) of the electrolyte was calculated according to the following equation:

$$\Lambda = 1000 \times K/C \quad (1)$$

where Λ is equivalent electrolyte conductivity at any concentration, *K* is specific conductivity, and *C* is standard or molar concentration of the acids under study.

Since the Schiff bases under study are weak electrolytes, it is not possible to directly find the equivalent conductivity value (Λ_o) at infinite dilution from the graph of the relationship between (Λ) and ($\sqrt{C}$). Therefore, these bases were converted to their corresponding sodium salts (Na_A) by titration with the standard base NaOH. Because the resulting sodium salts are strong electrolytes, the Kohlrausch equation was applied to them to obtain the values of (Λ_{oHA}).

$$\Lambda = \Lambda o - b\sqrt{C} \quad (2)$$

Using the (Λ_o) values of HCl and NaCl taken from reliable literature sources [27], the limiting equivalent conductivity of each weak Schiff base (A1, A2, and A3), denoted as (Λ_{oHA}), was determined by applying Kohlrausch's law of independent ion migration, according to the following equation:

$$\Lambda_{oNaA}+\Lambda_{oHCl} \rightarrow \Lambda_{oHA} + \Lambda_{oNaCl} \quad (3)$$

Where (Λ_{oNaA}) represents the limiting equivalent conductivity of the sodium salt of the acid, obtained from the graphical plot; (Λ_{oHCl}) is the limiting equivalent conductivity of the hydrochloric acid, also determined from the graphical plot. and (Λ_{oNaCl}) is the limiting equivalent conductivity of sodium chloride, obtained from the graphical plot; and ($\Lambda_{oHA)}$ is the limiting equivalent conductivity of the weak Schiff base acids, which is the required value to be determined. After determining the value of (Λ_o) for the Weak base, the degree of dissociation (α) was calculated from the ratio of the equivalent conductivity at a given concentration to the limiting equivalent conductivity:

$$\alpha = \Lambda/\Lambda_o \quad (4)$$

Where:
α = degree of dissociation of the weak electrolytes.
Λ = equivalent conductivity of the Schiff base at any concentration.
Λ_o = limiting equivalent conductivity of the base at infinite dilution.
Finally, the ionization constant (Ka) of the weak acid under study was determined using Ostwald's dilution law, as follows:

$$Ka = \alpha^2 C / 1 - \alpha \quad (5)$$

According to the literature reported by [28], electrolytes are generally classified into two categories. Strong electrolytes exhibit a linear relationship when the equivalent conductivity at constant temperature is plotted against the square root of concentration, whereas weak electrolytes show nonlinear curved behavior under the same conditions. Accordingly, and based on Equation (2), the following expression was expression was applied. As shown in Fig.s 3-5 and Tables 4-7.

Table 4. Equivalent conductivity values of sodium chloride and hydrochloric acid solutions at different temperatures.

Temperatures, K	Λ_o (HCl)	Λ_o(NaCl)
293	344.4	116.530
303	396.18	142.970
313	441.01	170.280
323	516.93	211.500
333	569.74	242.970

Table 5. Electrical conductivity, degree of dissociation (α), and ionization constant (Ka) of compound A1 in water

Conc. Equivlit$^{-1}\times10^3$	Temp., K	Λ_{equiv} ohm^{-1}cm^{2}equiv^{-1}	Λ_o ohm^{-1}cm^{2}equiv^{-1}	α	$K_a\times 10^8$	$\grave{K}_a\times10^8$
1	293	1.5	375.15	0.00399	1.6051	3.775
0.8		2		0.00533	2.2859	
0.6		2.66		0.00709	3.0385	
0.4		3.75		0.00999	4.0081	
0.2		7.4		0.01972	7.9384	
1	303	2	416.74	0.00479	2.3143	4.928
0.8		2.6		0.00624	3.1335	
0.6		3.5		0.00839	4.2527	
0.4		5		0.01199	5.8279	
0.2		8.8		0.02112	9.1103	

1	313	2.4	460.66	0.00521	2.7285	5.153
0.8		3		0.00651	3.4142	
0.6		4.1		0.00890	4.7953	
0.4		5.5		0.01194	5.7705	
0.2		9.7		0.02106	9.0586	
1	323	3	551.34	0.00544	2.9760	5.446
0.8		3.7		0.00671	3.6276	
0.6		4.9		0.00889	4.7813	
0.4		6.8		0.01233	6.1512	
0.2		12		0.02176	9.6847	
1	333	3.4	603.13	0.00564	3.2001	6.298
0.8		4.4		0.00729	4.2821	
0.6		5.5		0.00912	5.0357	
0.4		8		0.01326	7.1287	
0.2		14.5		0.02404	11.8430	

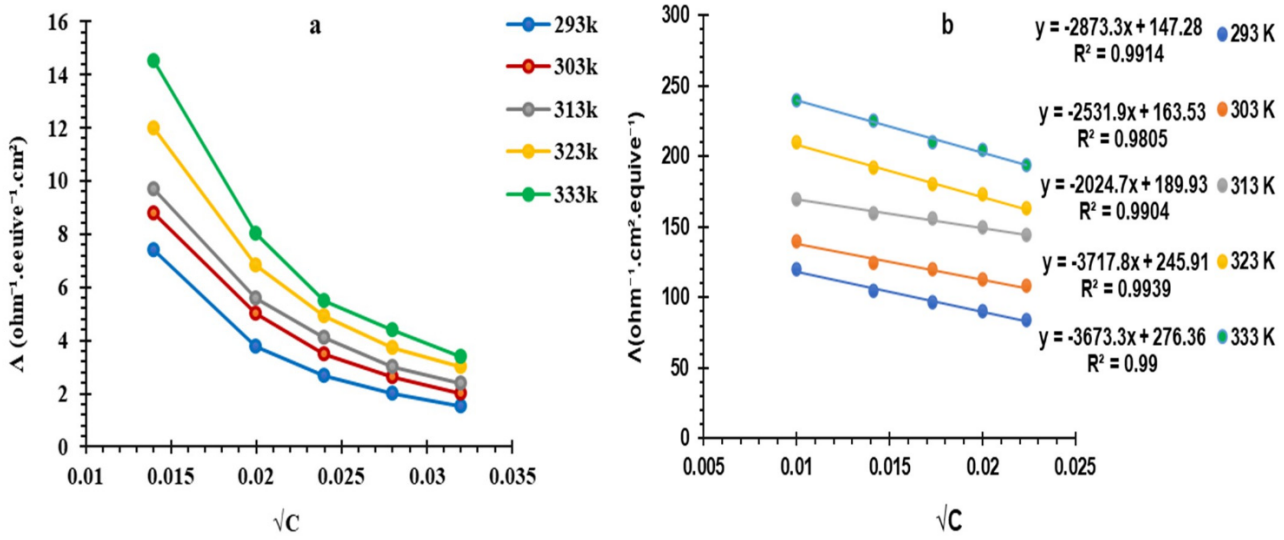

Fig. 3. Plot of (Λ) versus (√C) for compound A1 at different temperatures: (a) the weak acid exhibits a curved profile, (b) the sodium salt of the acid shows a linear behavior

Table 6. Electrical conductivity, degree of dissociation (α), and ionization constant (Ka) of compound A2 in water

Conc. Equivlit$^{-1}\times10^3$	Temp., K	Λequiv ohm^{-1}cm^{2}equiv^{-1}	Λ_o ohm^{-1}cm^{2}equiv^{-1}	α	$K_a\times10^8$	$\dot{K}_a\times10^8$
1	293	3.1	312.118	0.00993	9.963	17.621
0.8		3.7		0.01185	11.377	
0.6		4.4		0.01409	12.846	
0.4		6.5		0.02083	17.717	
0.2		13		0.04165	36.204	
1	303	4.1	398.68	0.01053	11.205	32.968
0.8		5.625		0.01411	16.155	
0.6		8.5		0.02132	27.866	
0.4		12.25		0.03073	38.971	
0.2		23		0.05769	70.637	
1		6.1		0.01430	20.745	
0.8		6.9		0.01617	21.261	

0.6	313	9.7	426.67	0.02273	31.719	40.115
0.4		13.5		0.03164	41.351	
0.2		27		0.06328	85.497	
1	323	7.7	475.39	0.01619	26.665	44.576
0.8		8.33		0.01872	28.574	
0.6		10.4		0.02187	29.358	
0.4		15		0.03155	41.121	
0.2		32		0.06731	97.160	
1	333	9.5	510.63	0.01860	35.252	58.266
0.8		11.7		0.02291	42.974	
0.6		14.333		0.02807	48.641	
0.4		19		0.03721	57.523	
0.2		36		0.07050	106.945	

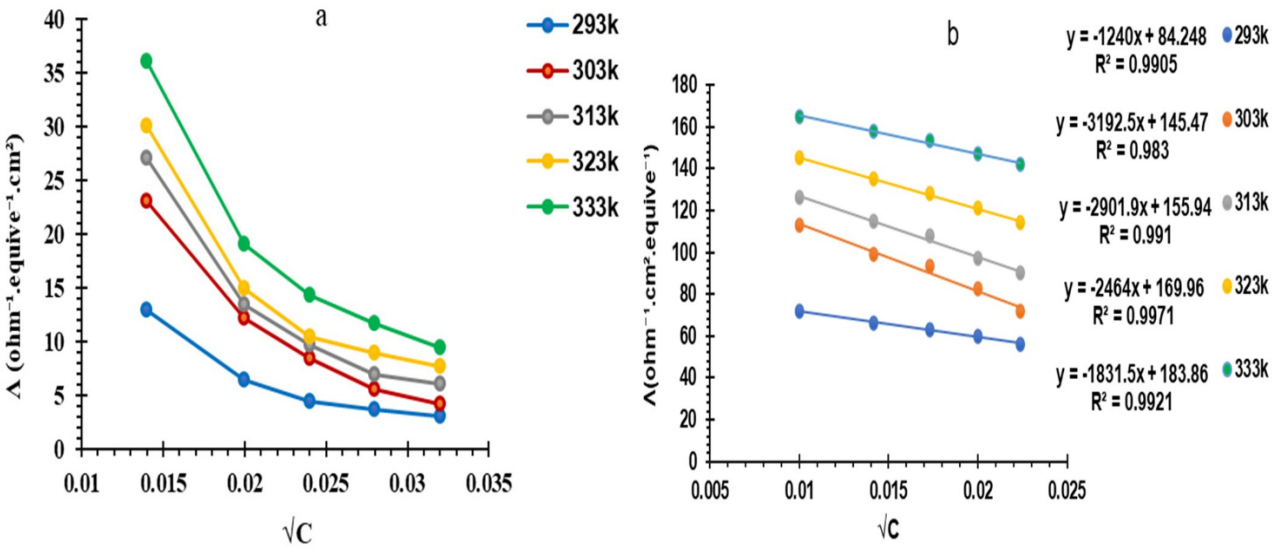

Fig. 4. Plot of (Λ) versus (√C) for compound A2 at different temperatures: (a) the weak acid exhibits a curved profile, (b) the sodium salt of the acid shows a linear behavior.

Table 7. Electrical conductivity, degree of dissociation (α), and ionization constant (Ka) of compound A3 in water.

Conc. Equivlit^{-1}×103	k	Λ_{equiv} ohm^{-1}cm^{2}equiv^{-1}	Λ_o ohm^{-1}cm^{2}equiv^{-1}	α	$K_a\times10^8$	$\grave{K}_a\times10^8$
1	293	2.6	364.66	0.00713	5.121	9.407
0.8		3.3		0.00905	6.616	
0.6		4		0.01097	7.299	
0.4		5.5		0.01508	9.238	
0.2		11		0.03017	18.765	
1	303	3.7	422.29	0.00876	7.745	14.219
0.8		4.75		0.01125	10.236	
0.6		5.83		0.01381	11.596	
0.4		7.7		0.01823	13.546	
0.2		15.5		0.03671	27.971	
1	313	4.2	440.9	0.00953	9.161	15.831
0.8		4.9		0.01134	10.406	
0.6		6.1		0.01384	11.646	
0.4		9		0.02041	17.015	

0.2		17		0.03856	30.925	
1	323	5	519.87	0.00962	9.339	17.797
0.8		6.125		0.01178	11.237	
0.6		8		0.01539	14.430	
0.4		11		0.02116	18.295	
0.2		21.5		0.04136	35.683	
1	333	5.7	581.11	0.00981	9.716	22.453
0.8		7		0.01205	11.750	
0.6		9.8		0.01687	17.357	
0.4		14.25		0.02452	24.658	
0.2		28		0.04819	48.784	

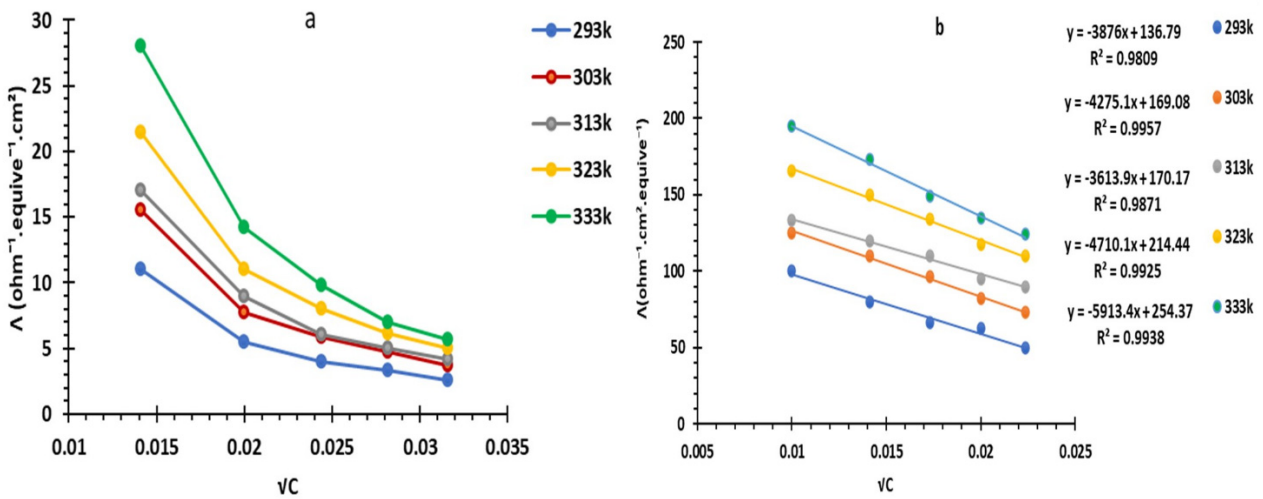

Fig. 5. Plot of (Λ) versus (√C) for compound A3 at different temperatures: (a) the weak acid exhibits a curved profile, whereas (b) the sodium salt of the acid shows a linear behavior.

The data listed in Tables 5-7 demonstrate that an increase in temperature leads to an enhanced degree of ionization for weak acids, resulting in a higher ionization constant (Ka). This observation indicates that the ionization process is endothermic. When comparing the acidity of the synthesized compounds at a constant temperature, a progressive increase in acidity is observed in the following order: (Km > Kp > Ko). The decrease in the ionization constant (Ka) at the ortho position is attributed to the formation of a strong and stable intramolecular hydrogen bond between the phenolic hydrogen and the azomethine nitrogen. This interaction stabilizes the proton and hinders its easy dissociation. In contrast, the para position exhibits moderate acidity, where the azomethine group withdraws electron density through both resonance and inductive effects, thereby stabilizing the phenoxide ion and facilitating proton loss. The highest ionization constant is recorded at the meta- position; this elevation is consistent with the absence of hydrogen bonding interference, allowing the strong inductive withdrawing effect of the azomethine group from a proximal position to effectively polarize the O-H bond and significantly enhance its dissociation [29, 30]. Since the acidity of the meta-isomer is higher than that of the para-isomer, this can be interpreted based on the sigma values in the Hammett equation. In the meta position, the hydroxyl group possesses a positive Hammett constant value (σ-meta = +0.12), indicating the dominance of the electron-withdrawing inductive effect in the absence of resonance participation. This reduces the electron density on the conjugated system, stabilizes the ionized state (phenoxide), and subsequently increases the Ka. Conversely, for the para isomer, the value (σ-para = ¯0.37) reflects the electron-donating resonance effect of the hydroxyl group, which increases the electron density and stabilizes the non-ionized form, leading to a decrease in the ionization constant compared to the meta position. This confirms that the position of the hydroxyl group determines the acidity through the competition between proton stabilization via intramolecular hydrogen bonding in the ortho position, and the inductive and resonance effects

manifested in the meta and para positions. Ultimately, all the aforementioned factors contribute to the overall increase in the acidity of the studied compounds [31].

Study of Thermodynamic Parameters. The obtained results were encouraging for the thermodynamic analysis. The Gibbs free energy change (ΔG°) for the ionization reaction was calculated at five temperatures using the relation:

$$\Delta G^\circ = -RTLnK_a \quad (6)$$

The enthalpy of ionization (ΔH°) of the acids was determined from the integrated Van't Hoff equation:

$$Ln\ Ka = constant - \Delta H / (RT) \quad (7)$$

The entropy change (ΔS°) for the ionization of the acids was calculated using the Gibbs equation:

$$\Delta G^\circ = \Delta H^\circ - T\Delta S^\circ \quad (8)$$

Plotting LnK_a versus 1/T yielded straight lines, as shown in Figure 6 for the acids under study, with correlation coefficients (R^2) ranging from 0.9651 to 0.9991, indicating excellent linearity.

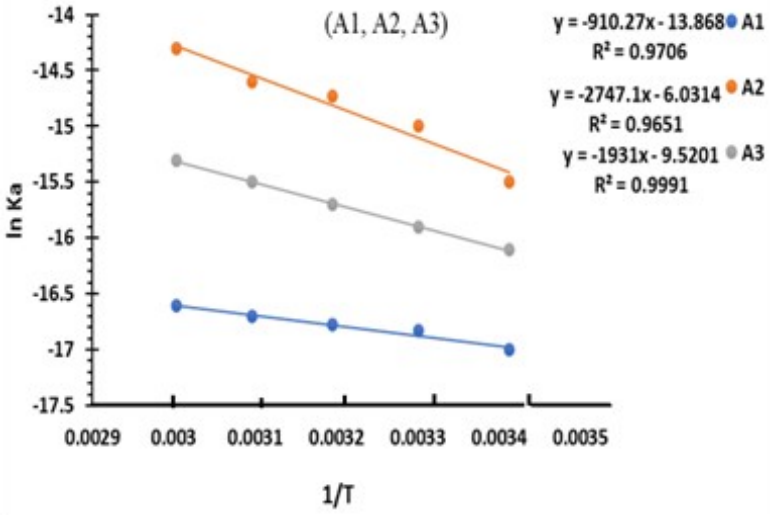

Fig. 6. Plot of lnK_a versus 1/T for the compounds A1, A2 and A3

Table 8. Thermodynamic parameters for the ionization reactions of the acids for the compounds at temperatures ranging from 293 to 333K.

Symbol	Absolute K temperature	ΔG J. mol^{-1}	ΔG` J. mol^{-1}	ΔH J. mol^{-1}	ΔH` J. mol^{-1}	ΔS J.mol^{-1}.K^{-1}	ΔS` J.mol^{-1}.K^{-1}
A1	293	+41643.45	+43704.81	+8165.47	+7941.65	-114.25	-114.25
	303	+42387.08		+7766.51		-114.25	
	313	+43668.89		+7905.73		-114.25	
	323	+44916.36		+8010.61		-114.25	
	333	+45908.29		+7859.94		-114.25	
A2	293	+37887.13	+38565.19	+23161.26	+22834.13	-50.25	-50.25
	303	+37598.19		+22369.72		-50.25	
	313	+38329.01		+22597.95		-50.25	
	323	+39268.92		+23035.28		-50.25	
	333	+39742.70		+23006.47		-50.25	
	293	+39412.07		+16212.81		-79.17	
	303	+39716.79		+15725.74		-79.17	

A3	313	+40746.53	+40798.69	+15965.52	+16016.22	-79.17	-79.17
	323	+41734.14		+16159.52		-79.17	
	333	+42383.91		+16017.51		-79.17	

From the results obtained in the above table 8, the following conclusions were drawn: The Gibbs free energy (ΔG°) for the ionization reactions is positive, indicating that the ionization processes are non-spontaneous. This is attributed to the phenolic acidic groups in the compounds, which contain covalent bonds that are difficult to ionize in water. The enthalpy change of ionization (ΔH°) is positive, confirming that the process is endothermic. In contrast, the entropy change (ΔS°) is negative, contrary to the theoretical expectation, where the entropy of the products typically increases relative to the ionizing species. The negative ΔS° arises from solvent interactions with the products, leading to an ordering of the resulting ions, or due to hydrogen bonding, particularly intermolecular hydrogen bonds. These thermodynamic observations are consistent with previous studies [32, 33].

Analysis of the Effect of Thermal Variation on Limiting Equivalent Conductivity Values. This section deals with the investigation and analysis of the response of the limiting equivalent conductivity (Λ_o) to systematic variations within a temperature range of (20-60 C°). This analytical evaluation was based on the mathematical model adopted [23], represented by the following equation (9):

$$\Lambda_{o(t)} = \Lambda_{o(25)} + B\Lambda_{o(25)} (t - 25) \quad (9)$$

Where ${}_o\Lambda_{(t)}$ is limiting equivalent conductivity of the solution at any temperature; $\Lambda_{o(25)}$ is limiting equivalent conductivity of the solution at 25 C°; *B* is thermal stability coefficient.

Upon plotting the relationship between $\Lambda_{o(t)}$ and (t – 25), straight lines were obtained with correlation coefficients ranging from 0.9636 to 0.9801. The results revealed a direct proportional relationship between the limiting equivalent conductivity and temperature. By calculating the values of the thermal stability coefficients (B), which are associated with the nature of the solution and its physical properties, according to Equation (9), the following values were obtained. As shown in Table 9 and Fig. 7.

Table 9. Results obtained from the application of Equation (9)

Compound	$\Lambda_{o(25)}$	B	R^2
A1	392.8	0.0150	0.9801
A2	353.69	0.0134	0.9636
A3	386.21	0.0137	0.9722

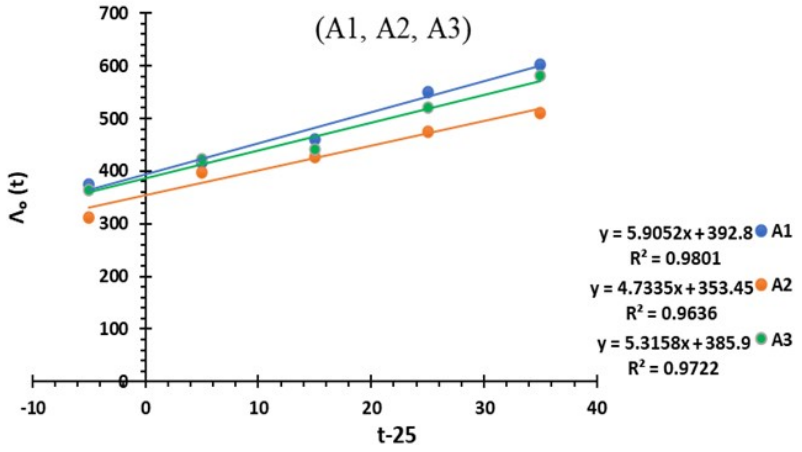

Fig. 7. Linear relationship between $\Lambda_{o(t)}$ and (t -25) for the studied compounds

Effect of Solvent on Ionization Behavior. Recent studies demonstrate [33] that water serves as an ideal medium for determining the ionization constants of acidic and basic compounds. This is primarily attributed to its high dielectric constant, which significantly diminishes the electrostatic attraction between oppositely charged ions, thereby facilitating. their separation in solution. This behavior is governed by the electrostatic interaction relationship (Coulomb's Law):

$$F = \frac{q1\ q2}{\varepsilon r^2} \quad (10)$$

Here:
F represents the electrostatic force between the ions;
q_1 and q_2 are the magnitudes of the charges;
ε is the dielectric constant of the medium;
r is the inter-ionic distance.

Thereby, according to this relationship, inversely proportional to the chemical bond, the reaction strength will be measured to the dielectric constant; therefore, increasing the value of (ε) results in a decrease in electrostatic attraction and is a beneficial factor to favor ionization. While water is effective on purpose as an ionizing medium, there are certain practical limitations because many acidic and basic organic compounds are poorly soluble. In order to avoid this, mixed solvent systems can be adopted, namely water-alcohol mixtures, which are employed to improve the solubility along the entire process without greatly impacting the ionization equilibrium. According to studies, the relative deviation caused by the presence of alcohol in the measured ionization constant (Ka) is negligible and almost constant, which is acceptable and relatively minor compared to the general trend and qualitative interpretation of the conclusions. Furthermore, specific solvation interactions, such as hydrogen bonding between the protic solvents and the azomethine nitrogen of Schiff bases, significantly contribute to the stabilization of the dissociated species alongside non-specific dielectric effects. As shown in Table 10, compound A1 is presented as an illustrative example of the ionization behavior of the other compounds studied.

Table 10. Electrical conductivity, degree of ionization (α), and ionization constant (Ka) of compound (A1) in alcohol

Conc. Equivlit$^{-1}\times10^3$	K	Λ_{Equiv} Ohm^{-1}cm^{2}equiv^{-1}	Λ_o Ohm^{-1}cm^{2}equiv^{-1}	α	$K_a\times10^9$	$\grave{K}_a\times10^9$
1	293	0.75	375.15	0.000266	0.071	0.481
0.8		1.06		0.000479	0.184	
0.6		1.5		0.000826	0.410	
0.4		2.5		0.001332	0.713	
0.2		4.8		0.002266	1.028	
1	303	0.82	416.74	0.000384	0.148	0.571
0.8		1.175		0.000528	0.231	
0.6		1.83		0.000912	0.499	
0.4		3		0.001439	0.839	
0.2		5.75		0.002399	1.154	
1	313	1	460.66	0.000434	0.188	0.732
0.8		1.63		0.000608	0.296	
0.6		2.58		0.000977	0.573	
0.4		4		0.001368	0.749	
0.2		8		0.003039	1.853	
1	323	1.4	551.34	0.000453	0.206	0.951
0.8		2		0.000726	0.421	
0.6		3.2		0.001034	0.642	

0.4		5		0.001451	0.843	
0.2		10		0.003628	2.642	
1		1.7		0.000663	0.440	
0.8		2.2		0.001011	0.819	
0.6	333	3.5	603.13	0.001359	1.110	1.606
0.4		5.7		0.001824	1.333	
0.2		12.8		0.004642	4.330	

The relative ionization constant (Kr) was calculated by a constant temperature and fixed molecular geometry for the acid. Here, the preference for alcohol molecules confirms the solvation of negative ions (conjugate base) over neutral species [34]. This means, quantitatively, the presence of a higher coordination number of solvent molecules surrounding the anionic species in addition to the non-ionized molecules. The dielectric is chosen to take in thermal fluctuation. Constant (D) of 100% ethanol was adjusted in Table 11 using the following empirical equation:

$$\text{Log } D = 1.3976 - 0.00264\ (t - 20) \quad (11)$$

The correlation between pKa and the dielectric constant (D) across the studied temperature range is illustrated in Fig. 8 [35]. The linear plots clearly demonstrate a direct proportional relationship between the pKa values and the dielectric properties of the medium at various temperatures.

Table 11. Comparison of the relative ionization constant (Kr) of the studied compounds in water and absolute ethanol at different temperatures

Compound	$\mathbf{Kr`} = \frac{\mathbf{Ka\ ethanol}}{\mathbf{Ka\ water}}$	T, K
A1	0.013	293
	0.012	303
	0.014	313
	0.017	323
	0.025	333
A2	0.0 25	293
	0.0 39	303
	0.0 32	313
	0.032	323
	0.026	333
A3	0.099	293
	0.131	303
	0.158	313
	0.152	323
	0.129	333

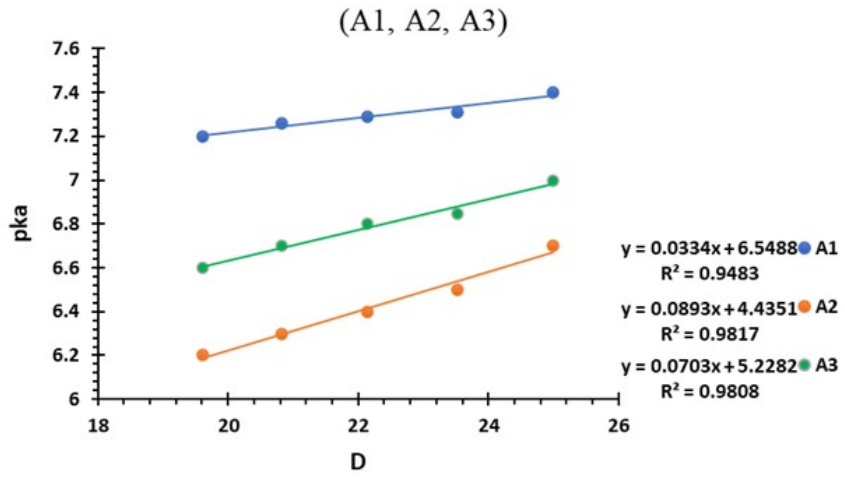

Fig. 8. Variation of pKa with the dielectric constant (D) for the studied compounds

The remarkable decrease in Ka and conductivity values in absolute ethanol compared to water is mainly attributed to its lower dielectric constant, which enhances the electrostatic attraction between ions and promotes ion-pair formation

Biological Study of the Prepared Compounds. Due to the well-established biological significance of Schiff bases, the preliminary antibacterial activity of the prepared compounds was investigated. The bacteria were studied because they cause the majority of diseases in hospitals and communities [36, 37]. The results showed promising activity. The antibacterial activity of the prepared Schiff base compounds was evaluated against *Escherichia coli* (Gram-negative) and *Staphylococcus aureus*, *Streptomyces lavendulae* (Gram-positive) using the agar wall diffusion method. Muller- Hinton agar plates were inoculated with bacterial suspensions prepared in normal saline. Subsequently, 30 µL of each compound solution was introduced into the while DMSO and gentamicin were used as negative and positive controls, respectively. The plates were incubated at 37 C° for 24 h, after which the diameters of the inhibition zones (mm) were measured [38, 39].

The gentamicin control exhibited inhibition zones of 13 and 20 mm against *Staphylococcus aureus* and *Streptomyces lavendulae* and 11 mm against *Escherichia coli*. The synthesized compounds showed promising antibacterial activity, with compound A1 exhibiting the highest activity against both bacterial strains, giving inhibition zones of 30 mm and 28 mm, respectively. Compound A2 showed the lowest activity (15 and 12 mm), whereas compound A3 demonstrated strong inhibition against *Staphylococcus aureus* (25 mm) and moderate activity against *Escherichia coli* (14 mm). The variation in antibacterial activity may be attributed to the nature and position of the functional groups in the Schiff base derivatives. Compound A1 was evaluated against Streptomyces lavendulae and showed an inhibition zone of 30 mm. Compounds A2 and A3 were not tested against this bacterial strain. As shown in Table 12 and Fig. 9.

Table 12. Inhibition zone diameters (mm) of the prepared Schiff bases against three bacterial strains

Symbol	*S. aureus*	*S. lavendulae*	*E. coli*
A1	30 mm	30mm	28 mm
A2	15 mm	------	12 mm
A3	25 mm	------	14 mm
DMSO	0mm	0 mm	0 mm

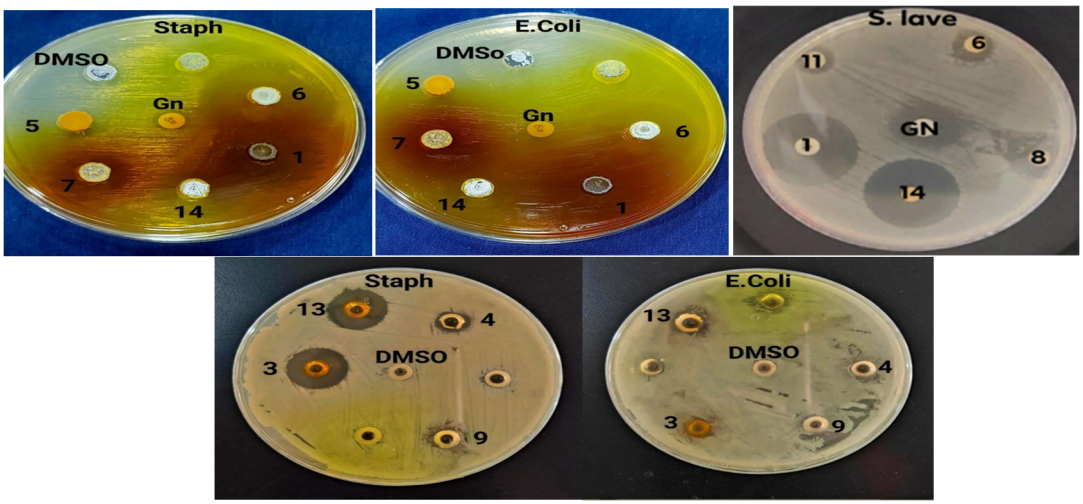

Fig. 9. Biological activity, A1=1, A2=4, A3=3

Molecular Docking Study. Molecular docking studies were performed to evaluate the binding interaction of the synthesized Schiff base with the biological target. The mitomycin resistance protein (AMRD protein), derived from Streptomyces lavendulae, was selected as the molecular target for this investigation. The crystal structure of this protein (PDB ID: 1KMZ) was retrieved from the protein data bank to explore the inhibitory potential of the prepared compounds at the molecular level. This protein is essential for the transport and metabolic processes within the bacterial cell, making it a significant target for antibacterial drug design [40, 41]. Identifying the most probable interaction sites was achieved through the CB-Dock2 platform's automated cavity detection.

We conduct molecular docking simulations to evaluate the binding of Schiff base compounds (A1-A3) to the target protein (PDB ID: 1KMZ), using gentamicin as a reference. The results showed that all derivatives can stabilize within the protein's active site in a close binding pattern. Compounds A1, A2, and A3 showed uniform binding capacity of -7.8 kcal/mol, meaning strong interaction compared to gentamicin (-6.0 kcal/mol). The means of stabilizing the bonds differed widely. Whereas the Schiff base complexes are largely stabilized by strong interactions between the aromatic rings ($\pi \rightarrow \pi^*$) stacking with the aromatic tryptophan residue Trp 108 (Fig. 11), gentamicin is stabilized by a network of hydrogen bonds to Arg72, Lys17, and Ser18, in addition to hydrophobic interactions with Val10, Val11, and Val12 (Fig. 10). This interaction is reinforced by the hydrophobic nature of the bonding pocket. The homogeneity of the docking results is in accordance with the common structure and electron density of the derivatives. Indeed, the present computational results are in agreement with the UV-Vis spectroscopic evidence of high electron density necessary for the compaction of the active molecules as defined by the $\pi \rightarrow \pi^*$ transitions.

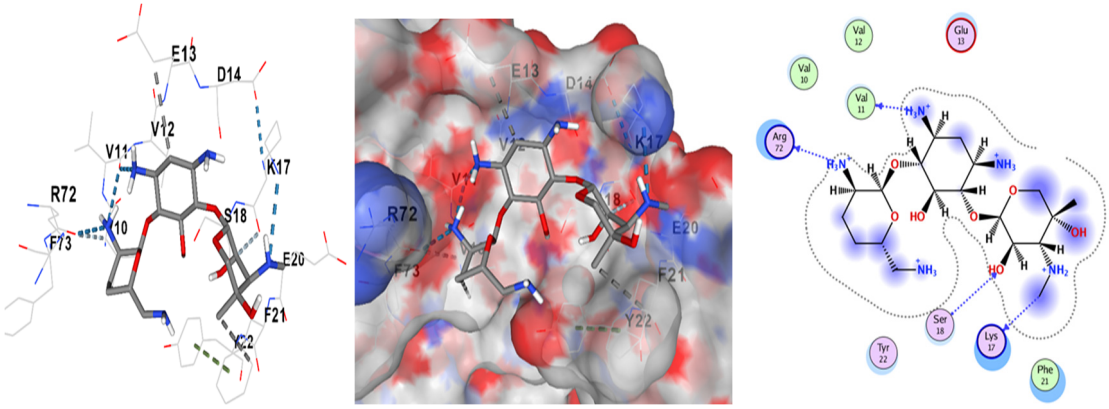

Fig.10. Molecular docking of the (Gentamicin) with protein (PDB: 1KMZ) in 3D and 2D.

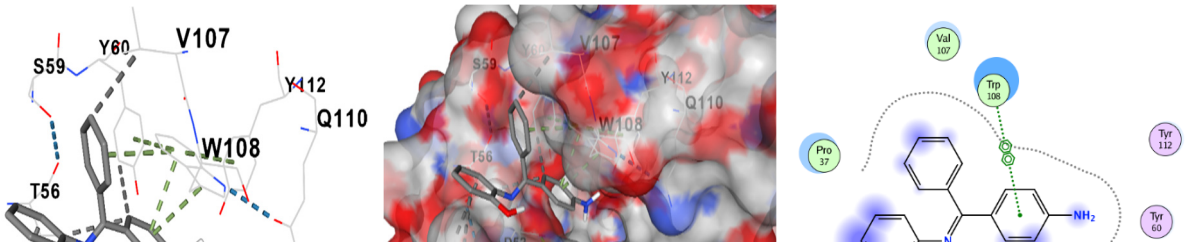

Fig.11. Molecular docking of synthesized Schiff bases (A1-A3) the with the Trp 108 (3D and 2D)

Correlation Analysis between Molecular Docking Scores and Biological Activity. The results of this study clearly show the correlation between the biological activity of prepared Schiff bases and molecular docking data and thermodynamic parameters. Despite the determined free energy values (ΔG+) showing that the ionization process is not spontaneous in the solution, the resulting compounds showed potent inhibition against the studied bacterial strains, especially compound A1, which had the highest inhibition rates. The difference is ascribed to the fact that biological activity does not directly depend on thermodynamic stability in solution but is more closely linked to the compound's ability to interact with the biomolecule. The analytical results of molecular docking confirmed the conclusion that the compounds possessed the best binding energy and the most compatibility with the active site of the protein, owing to their suppression activity. Meanwhile, the endothermic (ΔH>0) conditionality of the reaction and decrease in entropy (ΔS<0) at reaction temperatures lead to an increase in stability of the system due to increased ordering of the reaction structure of the complexes, reflecting, for example, a stable complex of ligand and protein formed for this binding process. Compound A1 is also much improved due to the hydroxyl group at an ortho position that enables the formation of intramolecular hydrogen bonds and stabilizes and enhances the spatial structure of the chemical group and lipophilicity to allow them to penetrate the bacterial cell wall and interact to activate the active site. In contrast, the meta-isomer A2 exhibits a weak electroeffect and a lack of resonance contribution, with an inactivation effect lower, whereas the para-isomer A3 has a positive resonance effect, resulting in moderate biological activity. Hence, it is mainly determined by the molecular interaction with biological target structure and spatial and electronic parameters and not mainly their solution thermodynamic value; thus, they conclude that the biological activity of the Schiff bases studied cannot be defined by the properties of the substrate itself. This emphasizes the significance of intermingling experimental and computational studies in order to achieve clear explanations of the actions of these compounds.

Conclusion

The results showed that the ionization constants increased with temperature, indicating enhanced acidity, while thermodynamic analysis confirmed an endothermic and non-spontaneous ionization process with decreased entropy. Biological evaluation revealed that compound A1 exhibited the highest antibacterial activity against both *Staphylococcus aureus* , *Streptomyces lavendulae,* and *Escherichia coli*, whereas docking results indicated strong binding interaction for all compounds. Overall, the results show that the produced Schiff bases possess promising physical, chemical, and biological properties, suggesting their potential use in further pharmaceutical research.

Acknowledgement

The Authors sincerely thank the Department of Chemistry at the College of Education for Pure Sciences, University of Mosul, Iraq, for providing the necessary laboratory facilities and instruments to conduct this research.

Conflict of interest

The authors declare no conflict of interest.

References

1. Abbas S.K., Hassan Z.M. Green chemistry approach for synthesis of Schiff bases and their applications. *Journal of Kerbala University*, 2025, **Vol. 22(1)**, p. 12-25
2. Rao D.P., Gautam A.K., Verma A., Gautam Y. Schiff bases and their possible therapeutic applications: a review. *Results Chem*. 2025, **Vol. 13**, 101941. DOI: 10.1016/J.Rechem.2024.101941
3. Thakur S., Jaryal A., Bhalla A. Recent advances in biological and medicinal profile of schiff bases and their metal complexes: an updated version (2018–2023). *Results Chem*. 2024, **Vol. 7**, 101350. DOI: 10.1016/J.Rechem.2024.101350
4. Abdulridha M.M., Hassan B.A., Baqer F.M. Design, Characterisation, molecular docking, and cytotoxicity study of new 5-Phenyl-4h-1, 2, 4-Triazole-3-Thiol Schiff bases derivatives. *Chemical Problems*, 2026, **Vol. 24 (4)**, 570. DOI: 10.65382/2221-8688-2026-4-570-581
5. Mushtaq I., Ahmad M., Saleem M., Ahmed A. Pharmaceutical significance Of Schiff bases: An overview. *Future J. Pharm. Sci*. 2024, **Vol. 10**, 16. DOI:10.1186/S43094-024-00594-5
6. Azadi S., Azizipour E., Amani A.M., Vaez A., Zareshahrabadi Z., Abbaspour A., Mosleh-Shirazi S. Antifungal activity of Fe_3o_4@ Sio_2/Schiff-Base/Cu (Ii) magnetic nanoparticles against pathogenic candida species. *Sci. Rep*. 2024, **Vol. 14**, 5855. DOI: 10.1038/S41598-024-56512-5
7. Wang F., Chen S., Liu J., Han Q., Ma X., He Z., Cheng X. Bent-core hexacatenar liquid crystals with diphenylmethane or benzophenone core and salicylaldimine arms: self-assembly and dual-modality fluorescence probe. *Dyes Pigments*, 2025, 113253. DOI:10.1016/J.Dyepig.2025.113253
8. Xue T., Li Y., Zhao X., Nie J., Zhu X. A facile synthesized benzophenone Schiff-base ligand as efficient type II visible light photoinitiator. *Prog. Org. Coat*. 2021, **Vol. 157**, 106329. DOI:10.1016/J.Porgcoat.2021.106329
9. Mustieles V., Balogh R.K., Axelstad M., Montazeri P., Márquez S., Vrijheid M., Andersson A.M. Benzophenone-3: Comprehensive review of the toxicological and human evidence with meta-analysis of human biomonitoring studies. *Environ. Int*. 2023, **Vol. 173**, 107739. DOI:10.1016/J.Envint.2023.107739
10. Van Nguyen D., Tran L.D., Vu P.U.N., Van Meervelt L., Nguyen M.N.T., Ngo A.L., Duong H.Q. Design, Synthesis, and biological evaluation of some novel o-aminophenol derivatives. *Curr. Org. Synth*. 2025, **Vol. 22**, p. 754-768. DOI:10.2174/0115701794360303250109065121
11. Li H., Li H., Wang M., Zheng Y., Li W., Hu J. Synthesis, Structure, and anticancer activity of ni (ii) complexes derived from polyhalogenated 2-aminophenol Schiff bases. *J. Inorg. Biochem*. 2025, 113139. DOI:10.1016/J.Jinorgbio.2025.113139
12. Masoodi H.R., Bagheri S. Effects of polar organic solvents and intramolecular hydrogen bond on stability, tautomerism, and electronic properties of Schiff bases: a dft study. *Inorg. Chem. Res*. 2025, **Vol. 9**, p. 46-53. DOI:10.22036/J10.22036.2025.506513.1182
13. Alizadeh K., Ghiasvand A.R., Borzoei M., Zohrevand S., Rezaei B., Hashemi P., Yavari I. Experimental and computational study on the aqueous acidity constants of some new aminobenzoic acid compounds. *J. Mol. Liq*. 2009, **Vol. 149**, p. 60-65. DOI:10.1016/J.Molliq.2009.08.007
14. Kılıç H. Uv/Vis Spectrophotometric determination of slow equilibrated n(1)-h missing deprotonation constant of a pyrimidine and thiopyrimidine: the final situation of the four pKa values. *Spectrochim. Acta A*. 2020, **Vol. 229**, 117867. DOI:10.1016/J.Saa.2019.117867

15. Ünal D., Aydoğdu S.N. Elucidating ionization behavior: potentiometric titration for precise determination of pka values in medicinal chemistry. *Pharmata*. 2024, **Vol. 4**, p. 46-50. DOI: 10.5281/Zenodo.11051303
16. Harjan A.M., Alabady F.M., Al-Bardi S.I.A. Ionization constants of oximes using HF and PM3 quantum methods. *Central Asian Journal of Medical and Natural Science*, 2024, **Vol. 5(3),** p**.** 340-350.DOI:10.51699/cajmns.v5i3.2448
17. Al-Healy F.M. Electrical conductance study of glutamic acid complex with [Mn (Iı)] in different solvents and temperatures. *The Eurasia Proceedings Of Science Technology Engineering And Mathematics*, 2020, **Vol. 11**, p. 20-28.
18. Atkins P.W., De Paula J., Keeler J. Atkins' physical chemistry. 12th ed. Oxford university press. 2023. p. 927.
19. El-Sonbati A.Z., El-Bindary A.A., Mansour N.M., El-Zahed M.M. Novel bivalent transition metal complexes based on a 2-amino-3-hydroxypyridine schiff base ligand: synthesis elucidation, antimicrobial evaluation, antioxidant and molecular docking studies. *Bmc Chemistry*, 2025, **Vol. 19(1),** p. 177. DOI: 10.1186/S13065-025-01561-8
20. Scotti L., Mendonca Junior F.J.B., Ishiki H.M., Ribeiro F.F., Singla R.K., Barbosa Filho J.M., Da Silva M.S., Scotti M.T. Docking studies for multi-target drugs. *Current drug targets*, 2017, **Vol. 18(5),** p. 592-604. DOI: 10.2174/1389450116666615082511 1818
21. Barani O., Shahraki S., Nezami Z.S., Delarami H.S., Sanchooli E. Unveiling the molecular association of novel benzohydrazide-substituted Schiff base complexes with human serum albumin. *Inorganic Chemistry Communications*, 2024, **Vol. 162**, 112200. DOI:10.1016/J.Inoche.2024.112200
22. Sarode S., Karande N., Danao K., Nagar A., Raut R. Solvent-free and eco-friendly synthesis of schiff bases and imines. *Integrating Chemistry, Clinical Practice, And Pharmacoepidemiology From Molecule To Population,* 2026, **Vol. 4**, p. 71.
23. AL-Hyali E.A., Al–Taai F.H., Othman S.S. Thermodynamic and Theoretical Studies of average Ionization Constants of a Number of Phenolic Schiff Bases Derived from Salicylaldehyde by Conductivity Measurements. *Journal of Education and Science*, 2018, **Vol. 27(3)**, p. 46-70.
24. Sıdır Y.G., Sıdır İ. The optical properties, UV-Vis. absorption and fluorescence spectra of 4-Pentylphenyl 4-n-benzoate derivatives in different solvents. *Journal of Fluorescence*. 2025, **Vol. 35,** p. 8269–8287. DOI:10.1007/S10895-025-04154-9.
25. Yassin N.A., Jumaa F.H. Preparation, characterization, antibacterial evaluation, laser activity, molecular docking, and liquid crystallinity studies of new tetrazole derivatives. *Chemical Problems*, 2026, **Vol. 24(3),** p. 499-511. DOI: 10.65382/2221-8688-2026-3-499-511.
26. Odularu A.T. Ease to challenges in achieving successful synthesized schiff base, chirality, and application as antibacterial agent. *Biomed Research International*, 2023, **Vol. 1**, 1626488. DOI:10.1155/2023/1626488
27. Al-Tai F.H.M. Determination of ionization constants of some compounds derived from benzoylacetone and dimedone. M. Sc. Thesis, University of Mosul, 2004, (in arabic).
28. Artemov V., Ryzhov A., Ouerdane H., Stevenson K. Ionization differences between weak and strong electrolytes: the role of protonic quantum effects as perturbed by dielectric relaxation spectroscopy. *The Journal of Physical Chemistry B,* 2021, DOI:10.26434/Chemrxiv-2021-V9l4m
29. Shahamirian M., Szatylowicz H., Krygowski T.M. How OH and O–groups affect electronic structure of meta-substituted and para-substituted phenols and phenolates. *Structural Chemistry*, 2017, **Vol. 28(5)**, p. 1563-1572. DOI:10.1007/S11224-017-0965-4
30. AL-Dabbagh M.G.A. Determination of pKa for some Schiff bases derived from benzaldehyde and amino phenols by conductivity measurement. *Journal of Education and Science*, 2018, **Vol. 27(1),** p. 1-15. DOI:10.33899/Edusj.2014.161534
31. Hadjeb R., Barkat D. Determination of acid dissociation constants of some substituted salicylideneanilines by spectroscopy. Application of the Hammett relation. *Arab. J. Chem*. 2017, **Vol. 10**, p. S3646-S3651. DOI:10.1016/J.Arabjc.2014.04.002

32. Ali Mohsin A.H., Al-Niemi H., Mahmoud M. Thermodynamic study for the stability of aromatic complexes formation derived from the reaction of 4-dimethyl amino benzaldehyde with diazotized dinitro aniline reagents. *Egypt. J. Chem*. 2022, **Vol. 65**, p. 421-437. DOI: 10.21608/Ejchem.2021.87003.4241
33. Merie F. A Study of the component formats effect on ionzation constants for several schiff's pyridine water and ethanol with variant temperature. *Egypt. J. Chem*. 2020, **Vol. 63**, p. 4975-4985. DOI:10.21608/Ejchem.2020.21228.2266
34. Azozus A.S., Marai F.H. Effect of ethanol and water solvents on the ionization constants of acids derived from benzoylacetone and dimedone. *Journal of Education And Science*. 2010, **Vol. 23(3),** p. 1-16. DOI: 10.33899/edusj.2010.58366.
35. Shcherbakov V.V., Artemkina Y.M., Akimova I.A., Artemkina I.M. Dielectric characteristics, electrical conductivity and solvation of ions in electrolyte solutions. *Materials*. 2021, **Vol. 14(19**), 5617. DOI:10.3390/Ma14195617
36. Saeed N.H., Ali R.T., Saied S.M. Computational study on the Estramustine (EMCYT) and its active metabolites anticancer drugs 17-α-estradiol and nornitrogen. *Results Chem*. 2025, **Vol. 18**, 102747. DOI:10.1016/J.Rechem.2025.102747
37. Abdulraheem L.R., Abdlaziz A.N., Ali M.H., Alalbadrany K.A. Synthesis, diagnosis, biological activity for some substituted tetrazole derived from methyl 2-(p-tolyl) benzoate. *Chemical Problems*, 2026, **Vol. 24(3)**, p. 451-464. DOI: 10.65382/2221-8688-2026-3-451-464
38. Xu F., Hu K., Mohsin A., Wu J., Su L., Wang Y., Chu J. Recent advances in the biosynthesis and production optimization of gentamicin: A critical review. *Synthetic and Systems Biotechnology*. 2025, **Vol. 10(1)**, p. 247-261. DOI:10.1016/J.Synbio.2024.11.003
39. Al-Barwari A.S. Divalent transition metal complexes with mixed of β-enaminone and n, o-donor ligands: synthesis, characterization and biological assessment. *Bull. Chem. Soc. Ethiop.* 2025, **Vol. 39**, p. 65-78 DOI: 10.4314/Bcse.V39i1.5
40. Katchalski-Katzir E., Shariv I., Eisenstein M., Friesem A.A., Aflalo C., Vakser I.A. Molecular surface recognition: determination of geometric fit between proteins and their ligands by correlation techniques. *Proceedings of the National Academy of Sciences*, 1992, **Vol. 89(6)**, p. 2195-2199.
41. Martin T.W., Dauter Z., Devedjiev Y., Sheffield P., Jelen F., He M., Derewenda U. Molecular basis of mitomycin C resistance in Streptomyces: structure and function of the MRD protein. *Structure*. 2002, **Vol. 10(7)**, p. 933-942. DOI:10.2210/Pdb1kmz/Pdb